5-10-2005

The Ccompton-Getting Effect Of Energetic Particles With An Anisotropic Pitch-Angle Distribution: An Application To Voyager 1 Results At ~85 AU

Ming Zhang

The Astrophysical Journal, 624:1038–1048, 2005 May 10

THE COMPTON-GETTING EFFECT OF ENERGETIC PARTICLES WITH AN ANISOTROPIC PITCH-ANGLE DISTRIBUTION: AN APPLICATION TO *VOYAGER 1* RESULTS AT ~85 AU

Ming Zhang
Department of Physics and Space Science, Florida Institute of Technology, Melbourne, FL 32901
Received 2004 October 10; accepted 2005 January 31

ABSTRACT

This paper provides a theoretical simulation of anisotropy measurements by the Low-Energy Charged Particle (LECP) experiment on *Voyager*. The model starts with an anisotropic pitch-angle distribution function in the solar wind plasma reference frame. It includes the effects of both Compton-Getting anisotropy and a perpendicular diffusion anisotropy that possibly exists in the upstream region of the termination shock. The calculation is directly applied to the measurements during the late 2002 particle event seen by *Voyager 1*. It is shown that the data cannot rule out either the model with zero solar wind speed or the one with a finite speed on a qualitative basis. The determination of solar wind speed using the Compton-Getting effect is complicated by the presence of a large pitch-angle distribution anisotropy and a possible diffusion anisotropy. In most high-energy channels of the LECP instrument, because the pitch-angle distribution anisotropy is so large, a small uncertainty in the magnetic field direction can produce very different solar wind speeds ranging from 0 to >400 km s^{-1}. In fact, if the magnetic field is chosen to be in the Parker spiral direction, which is consistent with the magnetometer measurement on *Voyager 1*, the derived solar wind speed is still close to the supersonic value. Given the uncertainty of the magnetic field direction, only the two lowest energy channels of the LECP instrument can give a definitive result for the solar wind speed. However, these channels contain very high levels of background from their response to isotropic cosmic rays. An uncertainty of just a few percent in the background level can entirely hamper the estimate of solar wind speed.

Subject headings: plasmas — solar wind — Sun: particle emission

1. INTRODUCTION

Direct observation of the solar wind termination shock is an important milestone of heliospheric exploration, because much of our understanding of phenomena in the inner heliosphere, for example, anomalous cosmic rays, is based on the assumed existence of such a shock. Recently, two experiment teams on the *Voyager* spacecraft, the Low-Energy Charged Particle (LECP) and the Cosmic Ray Subsystem (CRS), reported an enhancement of energetic particles at *Voyager 1* (~85 AU and ~N34°; Krimigis et al. 2003; McDonald et al. 2003). The event began in middle 2002 and lasted about 6 months, and it was seen at *Voyager 1* but not at *Voyager 2*, which was at 70 AU S24°. A second event starting in late 2003 was reported recently to have the same characteristics. The two papers agreed that the particle enhancement can be a signature of the termination shock but interpreted it in different ways. Krimigis et al. (2003) suggested that the particle event is produced by the termination shock moving inward and passing the spacecraft and moving out again. However, McDonald et al. (2003) argued that the particle enhancement is a precursor of the termination shock, similar to upstream particles observed in the foreshock region of Earth's bow shock. Magnetic field data measurements on *Voyager 1* did not record significant enhancement of the magnetic field, which is normally associated with crossing the shock into subsonic plasma (Burlaga et al. 2003). Radio and plasma wave observations (Gurnett et al. 2003) on *Voyager* also gave evidence contradicting the interpretation of the termination shock crossing.

The central piece of evidence that led Krimigis et al. (2003) to claim that *Voyager 1* has crossed the termination shock is the LECP anisotropy measurements during the event. Using the theory of Compton-Getting anisotropy, Krimigis et al. (2003) derived a solar wind plasma speed of essentially zero with upper limit <50 km s^{-1}. Such a small plasma speed can only be consistent with the interpretation that the termination shock has passed the spacecraft and was moving inward at ~150 km s^{-1}. However, the particle event is not a typical event to which one can easily apply the theory of Compton-Getting anisotropy to derive the plasma speed, for there is a strong field-aligned flow that can complicate the analysis.

It is the purpose of this paper to provide a theoretical calculation of flux anisotropy for energetic particles with an anisotropic pitch-angle distribution. The theory is directly applied to the anisotropy measurements obtained by the LECP on *Voyager 1* during the late 2002 particle event. Factors that may affect the uncertainty of the plasma speed determination are assessed.

2. THEORY

Measurements of particle flux I, the number of particles per unit time, area, solid angle, and energy range, is equivalent to measuring the particle distribution function as a function of particle velocity vector in the spacecraft reference frame ($\boldsymbol{v}$) because of the relationship (Birmingham & Northrop 1979)

$$I(\boldsymbol{v}) = \frac{v^2}{m} f(\boldsymbol{v}), \tag{1}$$

where v is the magnitude of $\boldsymbol{v}$ ($v = |\boldsymbol{v}|$), m the mass of the particle, and $f(\boldsymbol{v})$ is the particle distribution function. The equation of Birmingham & Northrop (1979) had an extra factor of 2, which should not be there. For an anisotropy measurement in any energy channel of an instrument, v and m are fixed, and thus the anisotropy measurement directly reflects angular variation of the distribution function.

Usually, only the particle distribution function as a function of particle velocity in the reference frame moving with the plasma $f'(\boldsymbol{v}')$ can be known. It can be written as harmonic expansion of velocity (e.g., Toptygin 1985, chap. 8)

$$f'(\boldsymbol{v}') = f_0'(v') + \frac{3\boldsymbol{v}' \cdot \boldsymbol{J}}{v'^2}, \tag{2}$$

where $\boldsymbol{v}'$ is particle velocity in the plasma reference frame, $v' = |\boldsymbol{v}'|$, $f_0'(v')$ is the isotropic part of the distribution function, and $\boldsymbol{J}$ is the streaming flux vector in the plasma reference frame. The harmonic expansion is truncated after the first order because only the first-order anisotropy is concerned here. Under the diffusion approximation (the validity of the approximation may be violated under the condition when there is a large anisotropy, but here it is used as a overall guidance and some modification is made below), the streaming flux may be written as

$$\boldsymbol{J} = -\kappa \cdot \nabla f_0'. \tag{3}$$

The diffusion coefficient tensor in the magnetic field coordinates is

$$\kappa = \frac{v'}{3}\begin{pmatrix} \lambda_\perp & r_g & 0 \\ -r_g & \lambda_\perp & 0 \\ 0 & 0 & \lambda_{||} \end{pmatrix}, \tag{4}$$

where $\lambda_\perp$ and $\lambda_{||}$ are particle mean free paths perpendicular and parallel to the local magnetic field direction, respectively, and r_g is the particle gyroradius. After substituting equations (4) and (3) into equation (2), the distribution function in the plasma reference frame becomes

$$f'(\boldsymbol{v}') = f_0'(v')\Big[1 - \lambda_\perp \hat{\boldsymbol{v}}' \cdot \nabla_\perp \ln f_0' - \lambda_{||} \cos\theta' \nabla_{||} \ln f_0' + r_g \hat{\boldsymbol{v}}' \cdot \big(\hat{\boldsymbol{b}} \times \nabla \ln f_0'\big)\Big], \tag{5}$$

where $\hat{\boldsymbol{v}}'$ is the unit vector of particle velocity $\boldsymbol{v}'$ and θ' is the particle pitch angle in the plasma reference frame. In the low-energy range of the LECP measurements where the particle gyroradius is small compared to the scale size of the particle density gradient, the last term in equation (5) can be dropped.

The particle distribution function in the spacecraft reference frame can be simply obtained by a Galilean transformation:

$$f(\boldsymbol{v}) = f'(\boldsymbol{v}'), \text{ with } \boldsymbol{v}' = \boldsymbol{v} - \boldsymbol{V}, \tag{6}$$

where $\boldsymbol{V}$ is the velocity of plasma. This means that the phase-space density of particles in the spacecraft frame is same as in the plasma frame, except that it is evaluated at a different particle velocity.

In the diffusion approximation, the anisotropy is usually small, so

$$f(\boldsymbol{v}) = f_0'(v')\big(1 - \lambda_\perp \hat{\boldsymbol{v}}' \cdot \nabla_\perp \ln f_0'\big)\big(1 - \lambda_{||} \cos\theta' \nabla_{||} \ln f_0'\big), \text{ with } \boldsymbol{v}' = \boldsymbol{v} - \boldsymbol{V}. \tag{7}$$

The first term in equation (7), the isotropic part of the distribution function in the plasma reference frame, is generally considered to have a power law $f_0'(v') \propto v'^{-2(\gamma+1)}$ for nonrelativistic particles. The quantity γ is the spectral index of differential energy (E) spectrum; i.e., $I \propto E^{-\gamma}$ (see eq. [1]), which can be determined by direct measurements. Because $v' = |\boldsymbol{v} - \boldsymbol{V}|$ depends on the angle between $\boldsymbol{v}$ and $\boldsymbol{V}$, $f_0'(v')$ gives rise to an anisotropy, which is commonly referred to as the Compton-Getting anisotropy. If $V = |\boldsymbol{V}| \ll v = |\boldsymbol{v}|$, a Taylor expansion of $f_0'(|\boldsymbol{v} - \boldsymbol{V}|)$ results in the amplitude of the first-order harmonic of the Compton-Getting anisotropy $\boldsymbol{A}_{\rm CG} = -\boldsymbol{V}[\partial \ln f_0'(v)/\partial v] = 2(\gamma + 1)\boldsymbol{V}/v$. The second term, $1 - \lambda_\perp \hat{\boldsymbol{v}}' \cdot \nabla_\perp \ln f_0'$, is due to the perpendicular diffusion anisotropy $-\lambda_\perp \nabla_\perp \ln f_0'$. The *Voyager 1* observation indicates that the perpendicular anisotropy may be small, so this term can remain as it is. The third term, $1 - \lambda_{||} \cos\theta' \nabla_{||} \ln f_0'$ from parallel diffusion, represents a pitch-angle distribution of particles. The *Voyager 1* observation shows that the anisotropy along the magnetic field is large. Correction to higher order than the diffusion approximation is needed, so the parallel diffusion anisotropy is replaced by a general function of particle pitch-angle $P(\cos\theta')$, thus yielding

$$f(\boldsymbol{v}) = f_0'(v')\big(1 - \lambda_\perp \hat{\boldsymbol{v}}' \cdot \nabla_\perp \ln f_0'\big)P(\cos\theta'), \text{ with } \boldsymbol{v}' = \boldsymbol{v} - \boldsymbol{V}. \tag{8}$$

The above modification of parallel diffusion anisotropy does not alter the amplitude of the anisotropies from the other two effects. $P(\cos\theta')$ is to be determined by fits to the actual measurement. Because of the scarcity of data points in the anisotropy measurement, the fitting function has to contain as few parameters as possible, so the following analysis takes a simple exponential form of $P(\cos\theta') = \exp(A\cos\theta')$, where A is a fitting parameter. The same pitch-angle distribution function was used in the analysis of Krimigis et al. (2003).

In deriving equation (8), it is assumed that the diffusion anisotropy is small. Since the Compton-Getting anisotropy is also small, a small diffusion anisotropy can make a large difference in solar wind speed determination. In fact, *Voyager 1* observed a moderately large anisotropy in the pitch-angle distribution. As shown below, A can be as large as 0.6. At such a level, the diffusion approximation is marginally applicable. Thus, the diffusion theory can only be used to give a guideline to what is expected if there is a diffusion anisotropy. If the parallel diffusion anisotropy is replaced by a pitch-angle distribution, the theory can be reliably extended to large pitch-angle anisotropies. The magnitude of the perpendicular diffusion anisotropy is completely uncertain. If it is small or zero, equation (8) should be quite good. In a few cases of the following analysis, the diffusion approximation is extended to somewhat moderate perpendicular diffusion anisotropy (only in the few lowest energy channels) to give an estimate of how much the perpendicular diffusion can potentially make a difference in estimating the solar wind speed. It is shown below that the perpendicular diffusion anisotropy is not the only uncertainty in the solar wind speed determination.

The perpendicular diffusion anisotropy amplitude in the second term of equation (8), $-\lambda_\perp \nabla_\perp \ln f_0'$, strongly depends on the source of particles for the event. Table 1 lists three possible sources and their expected diffusion anisotropy.

If the particles are anomalous cosmic rays accelerated by a spherical termination shock, the diffusion anisotropy upstream or downstream the shock listed in the Table 1 can be derived easily from the particle transport equation (Parker 1965),

$$\frac{\partial f_0'}{\partial t} = \nabla \cdot (\kappa \cdot \nabla f_0') - \boldsymbol{V} \cdot \nabla f_0' + \frac{1}{3}(\nabla \cdot \boldsymbol{V}) p \frac{\partial f_0'}{\partial p}. \tag{9}$$

TABLE 1
Possible Values of Perpendicular Diffusion Anisotropy

Source of Particle Enhancement	Diffusion Anisotropy
(1) Upstream anomalous cosmic rays	$-\lambda_\perp \nabla_\perp \ln f_0 = -3\boldsymbol{V}/\boldsymbol{v}$
(2) Downstream anomalous cosmic rays	$-\lambda_\perp \nabla_\perp \ln f_0 \approx 0$
(3) Solar or interplanetary energetic particles	$-\lambda_\perp \nabla_\perp \ln f_0 \approx 0$

For low-energy particles at large radial distances from the sun, the effects of gradient/curvature drift (r_g in the diffusion tensor, eq. [4]) and adiabatic cooling (last term in eq. [9]) can be neglected. A steady state spherical solution to equation (9) in the radial direction at large radial distance r yields $\kappa_r(\partial f_0/\partial r) - Vf_0 =$ constant, which is set to 0 from the boundary condition far upstream. κ_r is the radial diffusion coefficient, which is equal to $v'\lambda_\perp/3$ if the magnetic field is perpendicular to the radial direction. The same results have been obtained by Jokipii & Giacalone (2004) and Jokipii et al. (2004). In a simple way, the perpendicular diffusion anisotropy of upstream anomalous cosmic rays

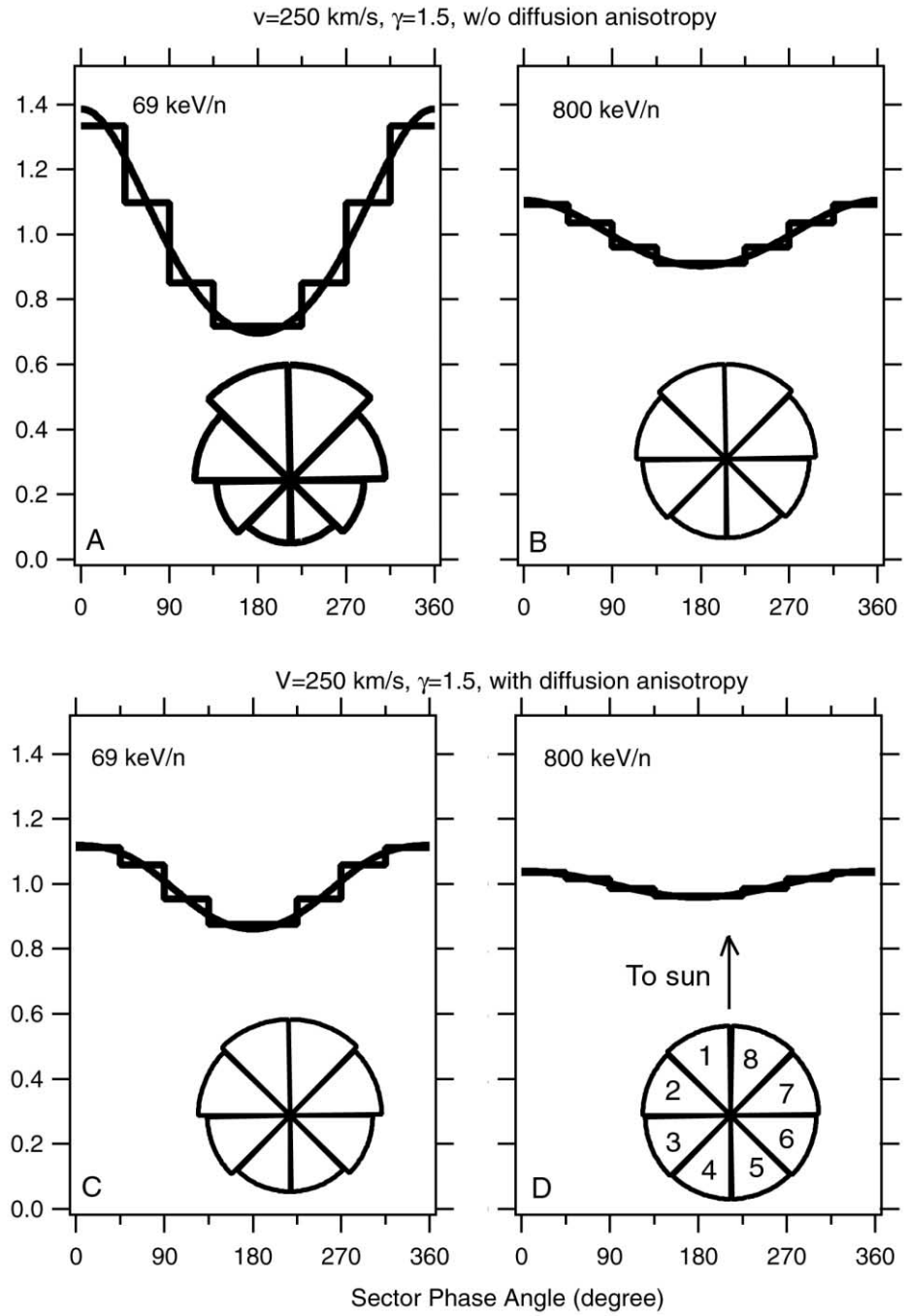

Fig. 1.—Calculation results of the angular variation of particle flux (*curves*) and its eight-sector averages (*histograms*) similar to the anisotropy measurement of the LECP instrument on *Voyager* for two different energies. The angular distributions of particle intensity are also shown as pie plots for easy comparison with other publications. In this case, the particle pitch-angle distribution function in the solar wind reference frame is isotropic ($A = 0$). The effect of diffusion anisotropy expected in the upstream region of the termination shock is shown in (*c*) and (*d*).

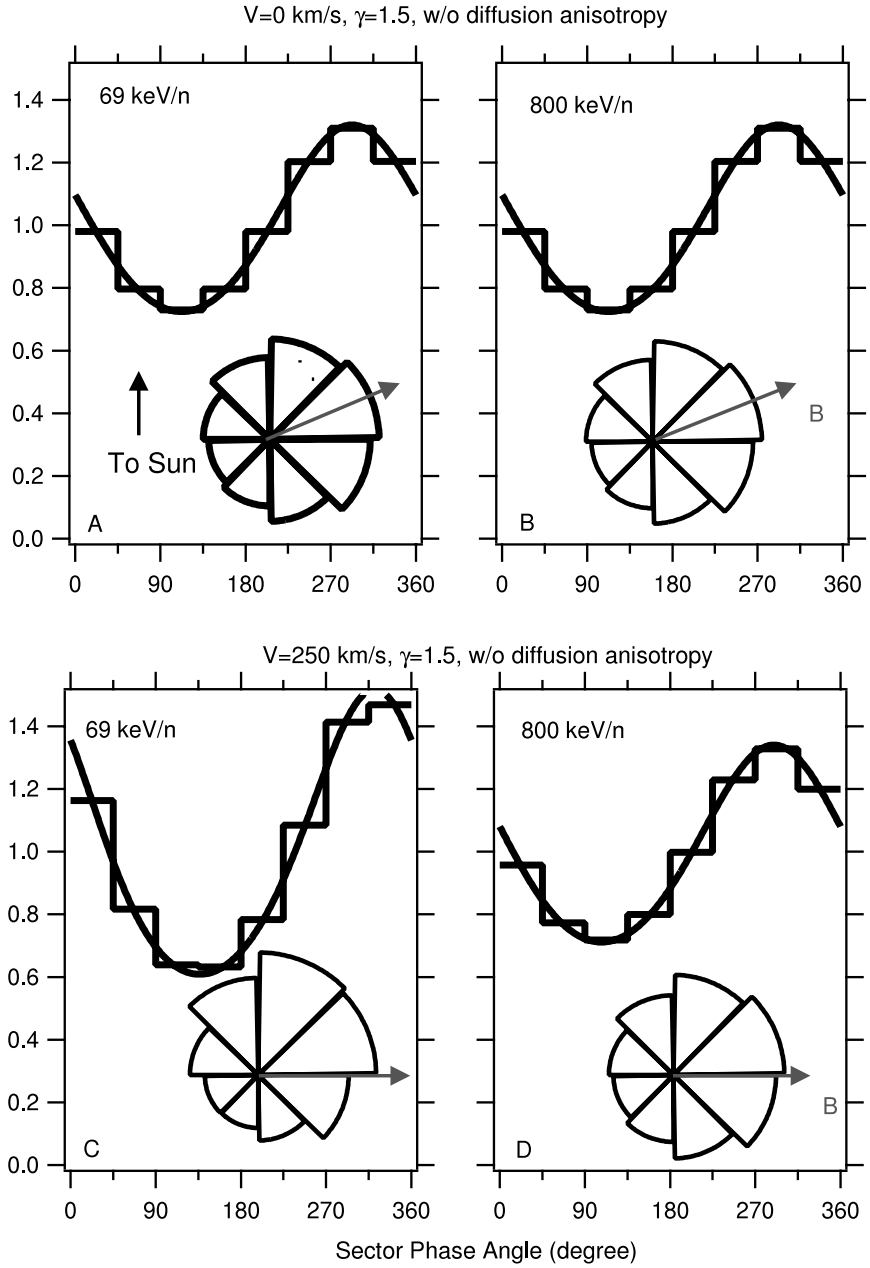

FIG. 2.—Calculation results of anisotropy measurement for two different sets of the magnetic field direction and solar wind speed when the particle pitch-angle distribution function in the solar wind reference frame is not isotropic ($A = 0.3$).

can be written as $-\lambda_\perp \nabla_\perp \ln f_0' = -3\boldsymbol{V}/v'$. If the particles are downstream anomalous cosmic rays, their transport is mainly through convection in equation (9) (see also Jokipii & Giacalone 2004), so the particle gradient and the perpendicular diffusion anisotropy should be 0.

If a nonspherical shock similar to the one in Jokipii et al. (2004) is considered, the particle gradient in the upstream region near the nose will remain roughly the same, but it may be smaller if the spacecraft is not at the nose, because particle transport parallel to azimuthally oriented magnetic field lines tends to spread the particles over a wider foreshock region and reduce the particle radial gradient. Therefore, the value for the upstream anomalous cosmic rays may serve as an upper limit for the perpendicular diffusion anisotropy.

The perpendicular diffusion anisotropy in the upstream region reduces the effect from the Compton-Getting anisotropy ($\boldsymbol{A}_{\rm CG}$), because they are in opposite directions, but the diffusion anisotropy cannot completely cancel or reverse the Compton-Getting anisotropy, provided that the particle spectral index γ is >0.5. Using the theory of Compton-Getting anisotropy without consideration of the diffusion anisotropy, one will underestimate the plasma speed by a factor of as much as $(2\gamma - 1)/(2\gamma + 2)$; for example, if the solar wind plasma speed is 300 km s^{-1} in the upstream region, one may get a speed as low as 120 km s^{-1} for a measured spectral index of 1.5. On the other hand, anomalous cosmic rays downstream of the termination shock only experience the Compton-Getting effect. The downstream solar wind speed is 100 km s^{-1} if the termination shock is a standing wave and has a compression ratio of 3. In a sense, the diffusion anisotropy tends to diminish the difference of particle anisotropy between upstream and downstream of the shock. This conclusion is consistent with the viewpoint of Jokipii & Giacalone (2004).

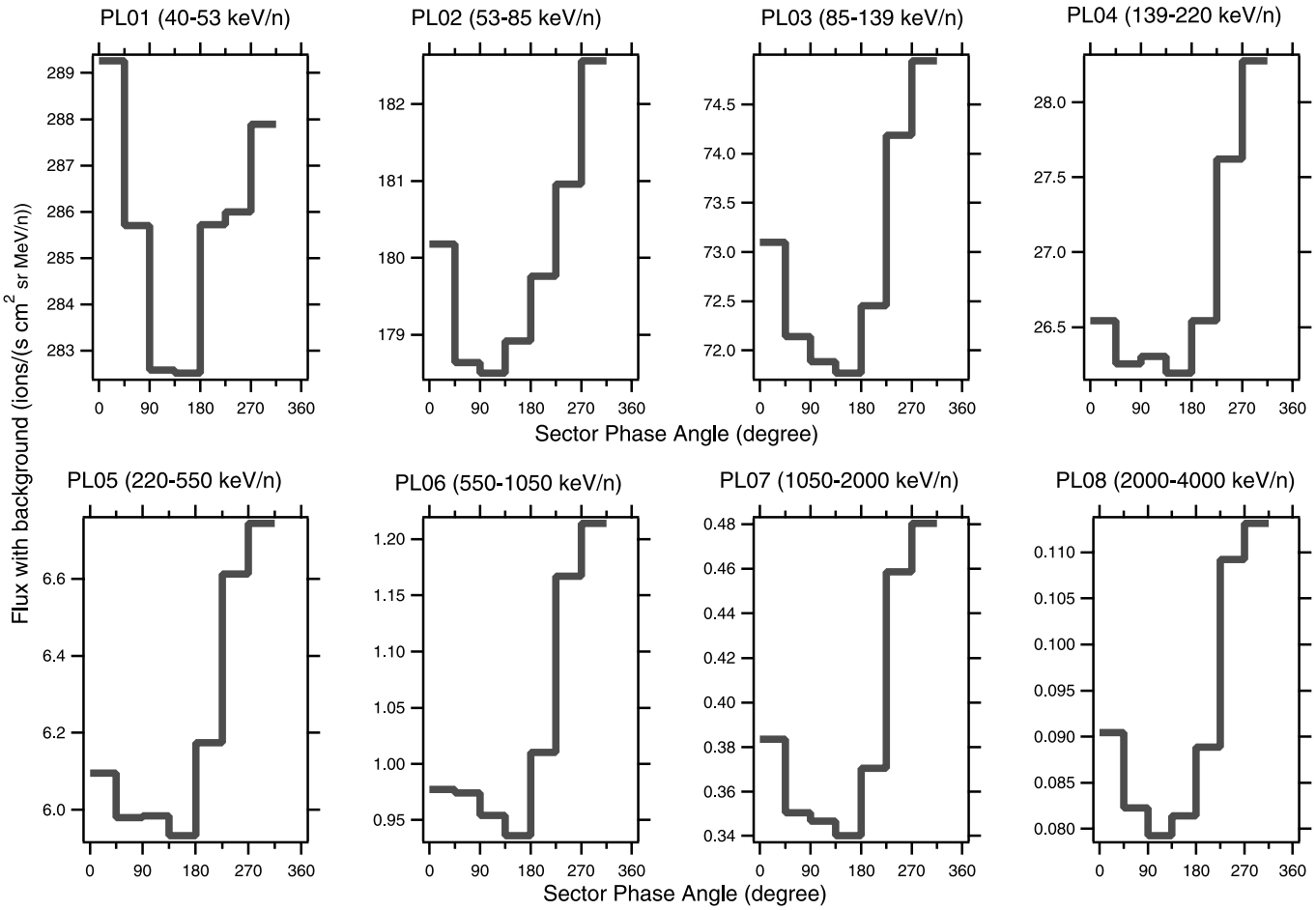

FIG. 3.—Angular distributions of particle intensity in eight ion channels measured by the LECP on *Voyager 1* for the entire particle event from day 195, 2002, to day 38, 2003.

If the particles are of solar or interplanetary origin, they must have diffused to a size much larger than the perpendicular mean free path after propagating to the large radial distance of the *Voyager 1* location and the diffusion anisotropy should be negligibly small.

The flux as a function of the direction of particle speed is calculated from equation (8) for two energies (fixed $v = |\boldsymbol{v}|$), one at 69 keV and the other 800 keV, corresponding to two of the LECP channels. Figures 1 and 2, which show the normalized flux versus the azimuth angle, give a few predictions for an 8 sector anisotropy measurement by a detector having a small field of view and scanning in the RT plane (a plane containing the radial and azimuth directions). The arrangement of the sectors is the same as the LECP measurement. The zero-degree azimuth angle is looking radially toward the sun. The particle flux in each of the sectors is proportional to the average value within a 45° angular range. Calculation for a detector with a large three-dimensional view cone can be done by integration, but the characteristics of the results is the same as that for a scanning detector with a small field of view. The result of the calculation is shown in two ways: sectored intensity as a function of azimuth phase angle and pie plot. The pie plot is used for easy comparison with the result in Krimigis et al. (2003), but the plot showing the intensity as a function of azimuth angle permits more detailed inspection of the angular variation.

When the particle pitch-angle distribution is isotropic in the plasma reference frame (Fig. 1), the Compton-Getting effect produces a distinguishing sunward-antisunward asymmetry with a flux minimum appearing in sectors 4 and 5 (Figs. 1*a* and 1*b*). Even when the upstream maximum perpendicular diffusion anisotropy is considered (Figs. 1*c* and 1*d*), the sunward-antisunward asymmetry remains although somewhat reduced, which is particularly true at the lower energy (Fig. 1*c*). This is because the Compton-Getting effect for particles with a spectral index of 1.5 still dominates the diffusion anisotropy.

However, the particle pitch-angle distribution for the late 2002 particle event seen by *Voyager 1* is not isotropic; i.e., $A \neq 0$ in equation (8). In this case, the magnetic field direction has to be given in order to make the calculation. Krimigis et al. (2003) assumed that the average magnetic field is directed parallel to the line at an azimuth angle of 292°.5 because of the apparent maximum of particle intensity in sector 7. Under such an assumption of magnetic field direction, a zero plasma speed is the best to fit the LECP measurements. In Figures 2*a* and 2*b*, minimum intensity appear in sector 3. The intensity in the sunward sector 1 is higher because it is closer to the maximum beam along the magnetic field direction.

Magnetic field measurements on *Voyager 1* indicates that the field direction is parallel to the line of azimuth angle 270°, as expected from the Parker spiral magnetic field at large radial distances. Figures 2*c* and 2*d* are results of calculation with a finite solar wind speed (250 km s^{-1}) and Parker spiral magnetic field direction. The overall features of intensity anisotropy are similar to Figures 2*a* and 2*b*. The Compton-Getting effect has a sunward-antisunward asymmetry. When it is added to the pitch-angle anisotropy along the Parker spiral, the total anisotropy

direction is shifted, resulting in a maximum intensity in sector 7. The minimum intensity appears in either sector 3 or 4, depending on the relative contribution from the Compton-Getting anisotropy and pitch-angle anisotropy. When the upstream perpendicular diffusion anisotropy is included, the overall behavior of the sector intensity distribution remains similar to Figures 2*c* and 2*d*.

The real magnetic field direction may fluctuate around its average significantly over the 6 month duration of the particle event. Take, for example, that the average magnetic field is in the Parker spiral direction and the magnetic field direction fluctuates in azimuth between -20° and 20° from its average with a uniform probability while the solar wind speed and pitch-angle anisotropy remain steady at $V = 250$ km s^{-1} and $A = 0.32$. The sectored intensities averaged over the entire range of magnetic field direction turn out to be almost the same as those shown in Figures 2*c* and 2*d*, which is calculated with a slightly smaller pitch-angle anisotropy $A = 0.30$. The average pitch-angle anisotropy gets smaller because the components of instantaneous pitch-angle anisotropy projected on to the direction perpendicular to the average magnetic field direction tend to cancel each other as the magnetic field direction fluctuates. Therefore, the effect of fluctuation of magnetic field direction can be neglected in data analysis unless the effect of particle streaming along the magnetic field is strongly biased toward some field directions in the long-term average.

3. DATA ANALYSIS

Figure 3 displays sectored intensity measurements obtained by the LECP on *Voyager 1*. The data is averaged over the entire particle event from day 195, 2002, to day 38, 2003. This time interval corresponds to pie plot B in the top section of Figure 3 in Krimigis et al. (2003). In this analysis, the long-term average is taken because (1) comparison with Krimigis et al. (2003) can be made easily, (2) statistical error of intensity measurements is small enough to warrant analysis, and (3) effect of coincidental magnetic field direction fluctuation is reduced. The plots are set to those vertical scales in order to highlight sector-to-sector variations. A sunward sector (sector 8) is shielded, so no data are shown. All eight energy channels contain a significant amount of background, although the intensities are expressed in units appropriate only for the true particles in their corresponding channels. Because the background most probably comes from response to isotropic higher-energy cosmic rays, a constant background needs to be subtracted from all the sectors in each of the energy channels.

The overall feature of the intensity variation in Figure 3 matches either of the predictions in Figure 2. Therefore, the anisotropy measurements by the LECP on *Voyager 1* cannot rule out either the model with zero solar wind speed or the one with a finite speed on qualitative basis. Any conclusion to be made about the solar wind speed must be based on quantitative analysis.

In order to obtain the solar wind speed from the anisotropy measurement the background has to be subtracted out because the speed depends on the absolute magnitude of anisotropy relative to the isotropic component. In the high-energy channels (PL04 or above), the background is less severe than those in low-energy channels. Take, for example, the PL06 550–1050 keV nucleon^{-1} ion channel, which has a rough match with the 0.53–1.78 proton channel shown frequently in Krimigis et al. (2003). The background constitutes roughly 60% of total counts in that channel, as indicated by the thick line at the bottom axis of Figure 4. After subtracting the background, its pie plot showing the angular distribution of 550–1050 keV nucleon^{-1} ions matches exactly the one published in Krimigis et al. (2003) paper. Best fits (*three almost identical curves*) to equation (8) yield three very different solar wind speeds depending on the choice of magnetic field direction and perpendicular diffusion anisotropy: (1) -43 km s^{-1} for a magnetic field direction at azimuth angle 292.°5 and no diffusion anisotropy (the same condition as that in Krimigis et al. 2003), (2) 279 km s^{-1} for a Parker magnetic field (270°) and without diffusion anisotropy, and (3) 739 km s^{-1} for a Parker magnetic field (270°) and with the maximum upstream perpendicular diffusion anisotropy. The error bar of solar wind speed from each of these three fits is much smaller than the differences among them. From this analysis, it can be concluded that, under the circumstance of a strong pitch-angle anisotropy, we cannot use the anisotropy measurement in this energy channel to determine the solar wind speed uniquely, because it is very sensitive to the choice of magnetic field direction and perpendicular diffusion anisotropy. This conclusion also applies to other high-energy channels (PL04 or above). This is because, at high energies, the Compton-Getting anisotropy in the typical solar wind is small, and thus it can be easily canceled out by a small uncertainty in the direction of a large pitch-angle anisotropy along the magnetic field.

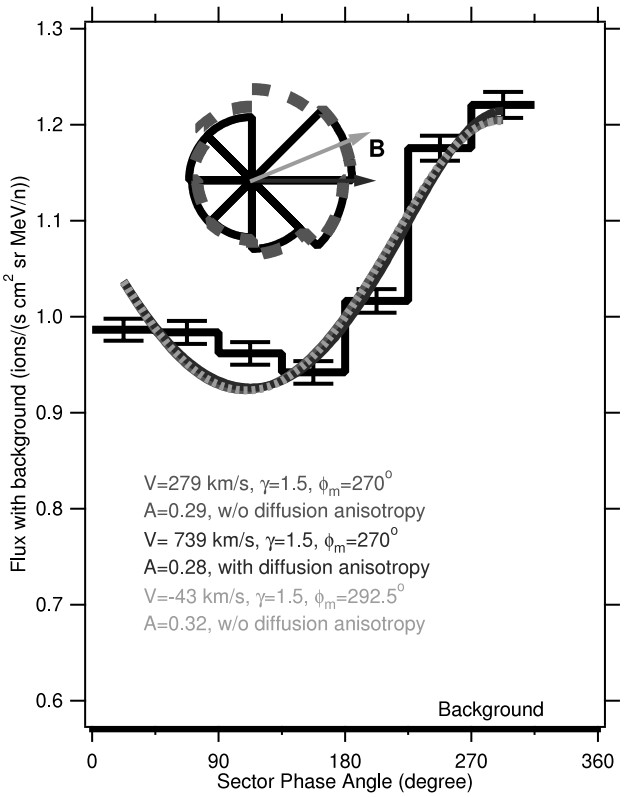

FIG. 4.—Fits (*curves*) to the anisotropy measurement (*histogram*) in the LECP PL06 channel yielding different solar wind speeds upon three choices of magnetic field direction and diffusion anisotropy. An isotropic background (*thick line at the bottom*) has been set at a level so that the pie plot matches the one in Krimigis et al. (2003).

The Compton-Getting anisotropy is expected to be stronger in low-energy channels like PL01 (40–53 keV) and PL02 (53–85 keV) of the LECP instrument. However, these channels contain a very high level of background from isotropic higher energy cosmic rays. Figure 5*a* show anisotropy measurement in the PL02 channel with a background set at the bottom of the plot, or ~90% of the total flux, to match the pie plot in Krimigis et al. (2003). After the background subtraction, best fits (three almost identical curves) to the PL02 sectored intensity with

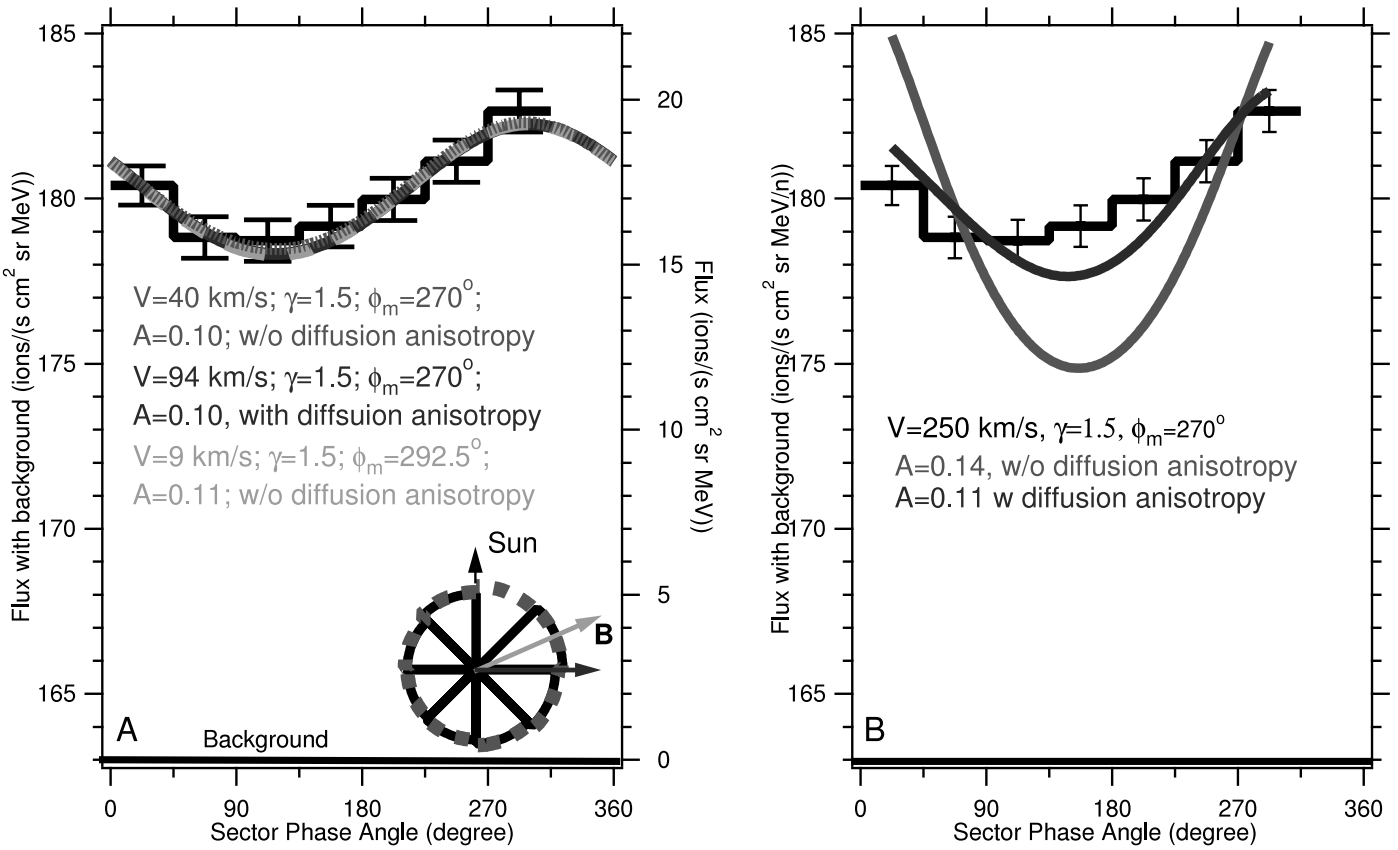

FIG. 5.—Fits (*curves*) to the anisotropy measurement (*histogram*) in the LECP PL02 channel yielding three solar wind speeds, depending on the choice of magnetic field direction and diffusion anisotropy (*a*). It is difficult to fit the measurement with a higher solar wind speed of 250 km s^{-1} no matter what magnetic field direction and diffusion anisotropy are taken (*b*). An isotropic background (*thick line at the bottom*) has been set at a level so that the pie plot matches the one in Krimigis et al. (2003).

equation (8) yield the following solar wind speeds: (1) 9 km s^{-1} for a magnetic field direction at azimuth angle 292.°5 and no diffusion anisotropy, (2) 40 km s^{-1} for a Parker magnetic field (270°) and without diffusion anisotropy, and (3) 94 km s^{-1} for a Parker magnetic field (270°) and with the maximum upstream perpendicular diffusion anisotropy. It is very difficult to fit the observations with a solar wind speed >250 km s^{-1}, even with the maximum upstream perpendicular diffusion anisotropy (Fig. 5*b*). This conclusion is quite robust if the background in Figure 5 has been determined within an uncertainty of ~5%.

To demonstrate the importance of the background determination in this analysis, let us raise the background by 8% to the level as shown by the bottom line in Figure 6. In this case, best fits of background-subtracted PL02 intensity yield three more different solar wind speeds: (1) 69 km s^{-1} for magnetic field direction at azimuth angle 292.°5 and no diffusion anisotropy, (2) 244 km s^{-1} for a Parker magnetic field (270°) and without diffusion anisotropy, and (3) 466 km s^{-1} for a Parker magnetic field (270°) and with the maximum upstream perpendicular diffusion anisotropy. A slightly smaller spectral index has been used for these fits because the particle spectrum becomes a little flatter after subtraction of additional background in low-energy channels (see below).

If some uncertainties (typically a few percent of total measurements in the four lowest energy channels) in the background determination are allowed, the LECP anisotropy measurements in all the energy channels can be fitted with a moderate solar wind speed (e.g., 250 km s^{-1}) given that the average magnetic field is in the Parker spiral direction (Fig. 7). For comparison, the

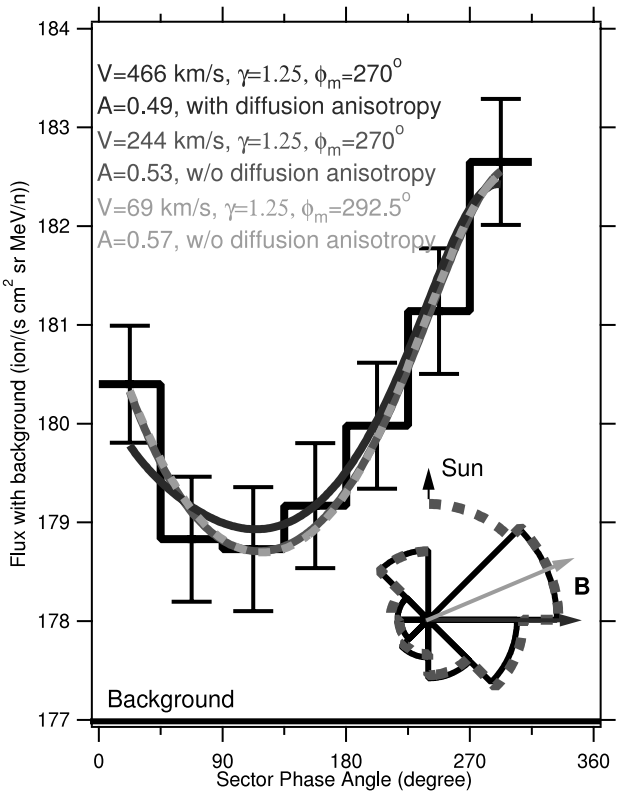

FIG. 6.—Fits (*curves*) to the anisotropy measurement (*histogram*) in the LECP PL02 channel after the background is set to a higher level. Three different solar wind speeds are obtained, depending on the choice of magnetic field direction and diffusion anisotropy.

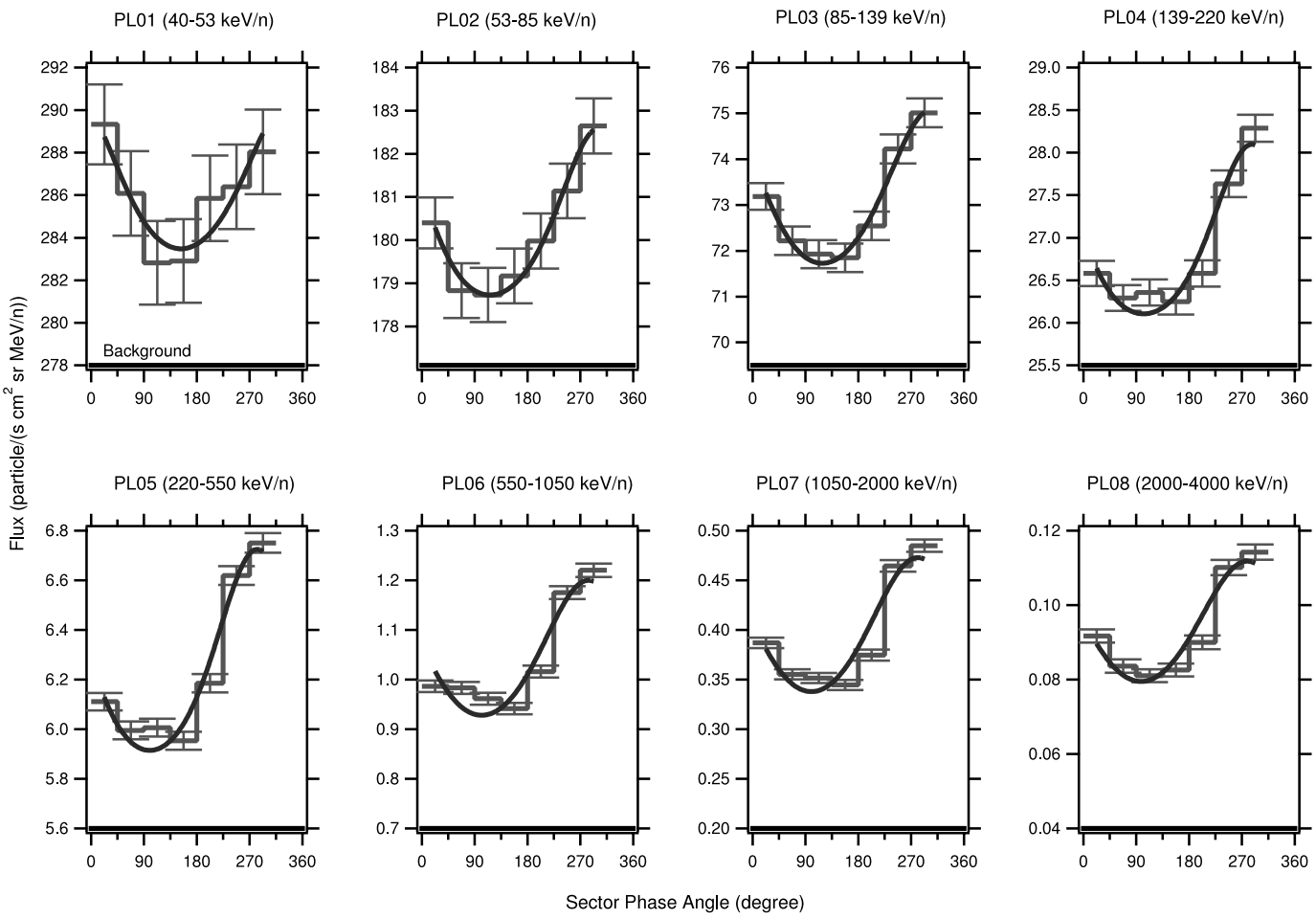

FIG. 7.—Fits (*curves*) to anisotropy measurements in all eight channels of the LECP instrument with a solar wind speed of 250 km s^{-1} with a Parker spiral magnetic field and a spectral index of 1.25. Diffusion anisotropy is set to zero.

background flux levels used in Figure 7 together with those deduced from Krimigis et al. (2003) are listed in Table 2. Note the determination of solar wind speed with high-energy channels is not very sensitive to the background subtraction mainly because of the smaller percentage of background contained in the channels, so the placement of the background in Figure 7 for the four highest energy channels is a little more arbitrary than in the lower-energy channels. The speed can be different if different background levels are set. It can be much larger if the upstream perpendicular diffusion anisotropy is present in the data.

TABLE 2

APPROXIMATE VALUES OF FLUX IN THE LECP CHANNELS

Channel	Total Flux	Background 1	Background 2
PL01	286	278	256
PL02	181	177	163
PL03	73.0	70.0	65.0
PL04	26.9	25.5	23.7
PL05	6.2	5.6	4.9
PL06	1.04	0.70	0.54
PL07	0.40	0.20	0.15
PL08	0.093	0.040	0.033

NOTES.—Background 1 is what is required in Fig. 7 to fit the anisotropy data with a 250 km s^{-1} solar wind speed. Background 2 is deduced from the graphs in Krimigis et al. (2003). Units are ions (s cm^2 sr MeV nucleon^{-1})$^{-1}$.

After subtraction of new background levels set in Figure 7, the omnidirectional ion spectrum (Fig. 8) gets slightly flatter than the one published in Krimigis et al. (2003). If the particles are upstream anomalous cosmic rays, a flatter spectrum is expected after propagation upstream to the spacecraft. On the other hand, if the spacecraft has passed in the termination shock, particle spectrum should keep the same shape from the shock, so a flatter spectrum means a higher shock compression ratio. Either way, the change of spectral shape is so minor that it will not affect the interpretations significantly.

4. DISCUSSION

The above analysis has shown that the determination of solar wind speed using the LECP anisotropy measurements on *Voyager 1* may contain uncertainties from the following factors: (1) assumption of magnetic field direction, (2) subtraction of background from cosmic rays, (3) presence of a possible diffusion anisotropy, as well as (4) the quality of fits to any particular model.

The last factor, 4, was addressed extensively in Krimigis et al. (2003). Our calculations have shown that the difference of best fits using different models is small. Therefore, the quality of fits is roughly the same for all the models. It should be pointed out that each LECP anisotropy measurement has only seven data points and fits to a model with too many free parameters are essentially meaningless.

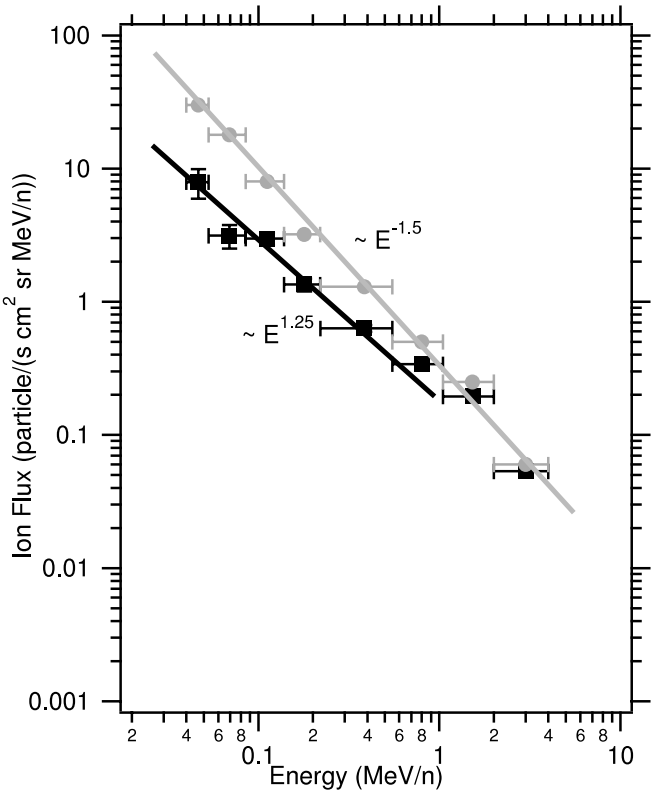

FIG. 8.—Energy spectrum of ions after subtraction of new background (*dark symbols*) set by Fig. 7. The spectrum in the light symbols is taken from Krimigis et al. (2003).

Jokipii & Giacalone (2004) have thoroughly discussed the contribution of a diffusion anisotropy that may exist upstream the termination shock, so this issue is not further elaborated here.

The determination of solar wind speed is quite sensitive to the magnetic field direction, particularly when using the high-energy particle channels. If the magnetic field direction is a free parameter, the fits produce solar wind speed error bars that are too large, so the magnetic field direction is chosen to be a semifree parameter in this analysis. Two configurations of the magnetic field are taken: Parker spiral magnetic field direction (parallel to the line of azimuth angle 270°), which is in agreement with *Voyager 1* magnetometer measurement and MHD theoretical expectation, and a field direction shifted from the Parker spiral sunward by 22°.5, which is to match the apparent particle intensity maximum in sector 7 of the LECP instrument. From the standard MHD theory point of view, it is very difficult to get the magnetic field in a remote solar wind shifted its direction from the Parker spiral by 22°.5 for a long period of time. It is even more difficult to explain if the spacecraft is downstream of the termination shock because the shock tends to amplify the azimuth component of the magnetic field in the solar wind by a ratio of shock compression while keeping the radial component the same.

The background determination in the two or three lowest energy channels holds a crucial position for the interpretation of postshock subsonic solar wind. If the previous background determination in Krimigis et al. (2003) has been made accurate within less than ~5% error bars, the derived low solar wind speed can be claimed. However, the measurements in the LECP low-energy channels consist mostly of the background from cosmic rays. For example, more than 90% of the PL02 is background, as one can see from its correction with the penetrating cosmic-ray intensity (EB05) in Figure 9. If a small percentage of background is missing, the solar wind speed will be underestimated quite a lot.

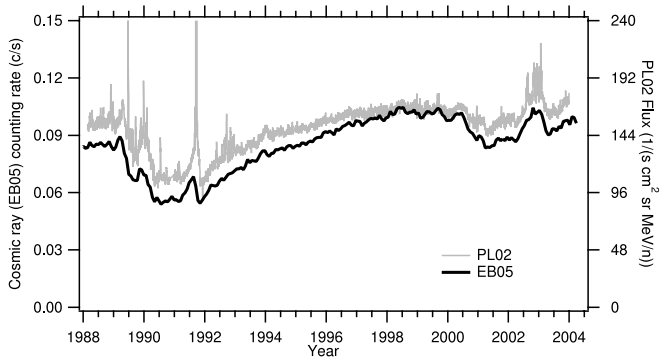

FIG. 9.—Time variations of daily measurements in the omnidirectional PL02 channel (*light curve*) and 26 day averages of the EB05 penetrating cosmic-ray counting rate (*dark curve*).

Unfortunately, the exact background subtraction procedure is not known to the author. Private communications with the LECP team reveal that the background subtraction does not employ the measurement in sector 8 that is shielded with 2 mm thick aluminium. The shielding material may alter the spectrum and intensity of cosmic rays arriving at the detector, so the measurement in the shielded sector cannot directly serve as background level. In addition, there is a radioactive source inside the shield; the actual counting rate in the shielded sector is often higher than those in the other sectors. Instead, a preferred background subtraction involves the measurements of high-energy cosmic rays, presumably the EB05 channel that measures penetrating particles above 60 MeV. Obviously from the example in Figure 9 the background in any of the low-energy channels is not necessarily linearly proportional to the EB05 counting rate. Take two time periods during which it is certain that the spacecraft was in the supersonic solar wind: one from day 19 to day 64 in 1998 and the other from day 19 to day 64 in 2002 (Krimigis et al. 2003). Fits to PL02 anisotropy measurements during these periods with the Compton-Getting effect from a solar wind of 300 km s^{-1} require that more than 98% of the PL02 channel counts should come from cosmic-ray background as indicated by the thick lines at the bottom in Figure 10. If the background is proportional to the EB05 counting rate and normalization ratio is set to match the true background level in 1998, then the time variation of background level is shown by the dark curve in Figure 11*a*. In this case, the background in the PL02 channel averaged over the entire late 2002 particle event (*thick bar*) is at 163 particles (s cm^2 sr MeV nucleon^{-1})$^{-1}$, which is consistent with what is used in Figure 5 and also by Krimigis et al. (2003). Clearly, such a normalization will not work for the period from day 19 to day 64 in 2002, because it predicts too little background. However, if the normalization ratio is set so that the background determination is correct for the early 2002 period (Fig. 11*b*), the background for the late 2002 particle event is raised to ~178 particles (s cm2 sr MeV nucleon^{-1})$^{-1}$, which is consistent with Figure 6. The difference of the background between the two settings is already more than 8%. Therefore, the normalization cannot be kept as a constant over different conditions of cosmic-ray background. It should be changing with the shape of cosmic-ray spectrum as well as the integral cosmic-ray intensity. A background subtraction procedure using merely the integral cosmic-ray counting rate cannot be adequate for a very accurate determination of the background,

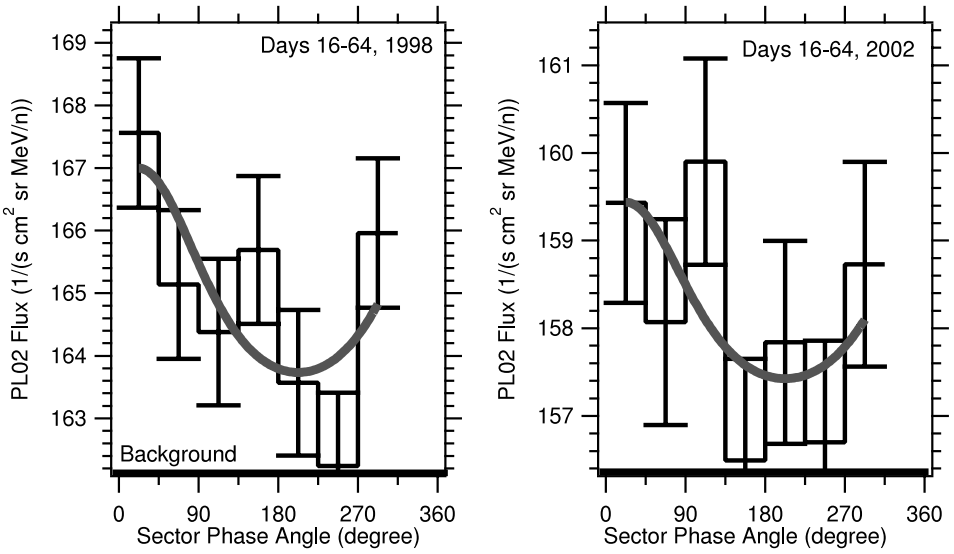

FIG. 10.—PL02 anisotropy measurements during two periods in early 1998 and 2002 and their fits to the Compton-Getting anisotropy with a solar wind speed of 300 km s^{-1}. The fits (*curves*) require that the background of the channel be set to the levels as shown by the thick lines at the bottom. More than 98% of the PL02 channel counts come from cosmic-ray background.

even though a nonlinear dependence on the integral cosmic-ray counting rate may be employed, because the cosmic-ray spectrum can vary significantly. On the other hand, if the shape of the cosmic-ray spectrum remains the same while the intensity is changing, the background should be proportional to the integral cosmic-ray counting rate. Because the cosmic-ray spectrum in the late 2002 particle event is more similar to that in early 2002 than that in 1998 (McDonald et al. 2003), the normalization used in Figure 11*b* is more appropriate. This seems to argue that the true background level for the late 2002 event should be closer to what is shown in Figure 11*b*, which is higher than that in Krimigis et al. (2003). In addition, the late 2002 particle event is a unique event: not only is the cosmic-ray ion spectrum very different from other events, but also there is an enhancement in cosmic-ray electrons (McDonald et al. 2003). Given these new conditions, it is a very stringent requirement to make the background determination have a better than ~5% error bar.

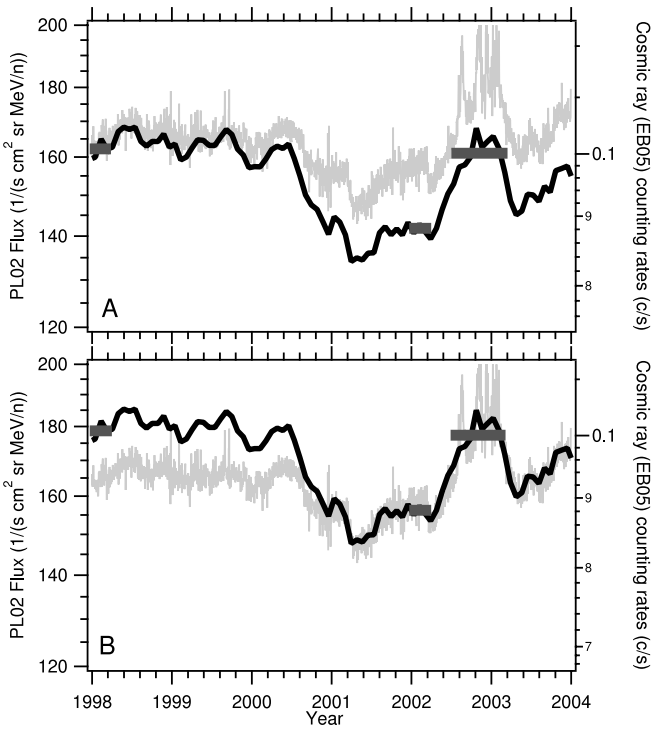

FIG. 11.—Time variations of daily measurements in the omnidirectional PL02 channel (*light curve*) and 26 day averages of the EB05 penetrating cosmic-ray counting rate (*dark curve*). The vertical scales of the EB05 counting rate have been set to match the correct background levels in 1998 (*a*) and early 2002 (*b*). If the background in the PL02 channel is proportional to the EB05 penetrating cosmic-ray counting rate, the dark curves in (*a*) and (*b*) indicate different levels of background during the particle event in late 2002. The thick horizontal bars show the average value of the background over the three time intervals.

5. SUMMARY

The first-order anisotropy of energetic particles observed by *Voyager 1* at ~85 AU contains at least two contributions: anisotropy of pitch-angle distribution along the magnetic field and the Compton-Getting anisotropy primarily in the radial direction. There is also a possibility of anisotropy from perpendicular diffusion if the particles are upstream anomalous cosmic rays (Jokipii & Giacalone 2004). Given these factors, one has to be extremely careful in using the Compton-Getting effect to derive solar wind speed, because it is difficult to separate out all the possible contributions to the anisotropy.

Anisotropy data obtained by the LECP on *Voyager 1* cannot rule out either the model with zero solar wind speed or the one with a finite speed on qualitative basis. Any conclusion about the solar wind speed must be based on quantitative analysis.

In most high-energy channels of the LECP measurements, the determination of the solar wind speed is very sensitive to the direction of magnetic field. Under the presence of strong field-aligned anisotropy, any deviation of the magnetic field from the Parker spiral direction can mimic or cancel the Compton-Getting anisotropy entirely. The uncertainty of magnetic field direction can bring a large uncertainty to the solar wind speed determination. The error bars of the derived solar wind speed are too large to tell whether it is possibly supersonic or subsonic.

Given the uncertainty of the magnetic field direction, only the lowest energy channels of the LECP instrument, in which the magnitude of Compton-Getting anisotropy can rival the pitch-angle

anisotropy, can put a definitive estimate of the solar wind speed. However, these channels contain very high level of background from their response to isotropic cosmic rays. An uncertainty of just a few percent in the background level can entirely hamper the estimate of solar wind speed. A more rigorous determination of the instrument background is needed. However, the anisotropy measurements in the lowest energy channels may hold to support the claim that *Voyager 1* has passed the termination shock only if it turns out that the background subtraction in the previously published data (Krimigis et al. 2003) has been accurate enough (error $<5\%$).

The author wishes to thank Robert Decker and Alan Cummings for useful discussion on the method of background determination. The work is supported in part by NASA Grants NAG5-10888, NAG5-11036, and NAG5-13514.

REFERENCES

Birmingham, T. J., & Northrop, T. G. 1979, J. Geophys. Res., 84, 41
Burlaga, L. F., Ness, N. F., Stone, E. C., McDonald, F. B., Acuña, M. H., Lepping, R. P., & Connerney, J. E. P. 2003, Geophys. Res. Lett., 30, 9
Gurnett, D. A., Kurth, W. S., & Stone, E. C. 2003, Geophys. Res. Lett., 30, 8
Jokipii, J. R., & Giacalone, J. 2004, ApJ, 605, L145
Jokipii, J. R., Giacalone, J., & Kóta, J. 2004, ApJ, 611, L141
Krimigis, S. M., Decker, R. B., Hill, M. E., Armstrong, T. P., Gloeckler, G., Hamilton, D. C., Lanzerotti, L. J., & Roelof, E. C. 2003, Nature, 426, 45
McDonald, F. B., Stone, E. C., Cummings, A. C., Heikkila, B., Lal, N., & Webber, W. R. 2003, Nature, 426, 48
Parker, E. N. 1965, Planet. Space Sci., 13, 9
Toptygin, I. N. 1985, Cosmic Rays in Interplanetary Magnetic Fields (Dordrecht: Reidel)